ES Materials and Manufacturing
DOI: https://dx.doi.org/10.30919/mm1480

Optimizing Waste Motor Oil Recycling into Diesel Using Novel Deep Eutectic Solvents: An Atomistic Study

Sagynysh Nurmanova,[1] Sergey Kolisnichenko,[1] Umirzhan Kokayev,[2] Dinara Kalmanova,[2] Abdikarim Karazhanov,[2] Zhassulan Alipbayev,[2] Fatima Abuova,[2] Omirzak Abdirashev[2,*] and Balzhan Satanova[2,*]

Abstract

The optimization of recycling processes for waste motor oil (WMO) into diesel fuel is crucial for sustainable waste management and resource recovery. This study explores the application of novel deep eutectic solvents (DES), specifically methyltriphenylphosphonium chloride (MTPPCl) and ethylene glycol (EGL)-based DES, for the efficient removal of naphthalene from WMO. Density functional theory (DFT) calculations and classical all-atom molecular dynamics (MD) simulations were employed to investigate the intermolecular interactions between DES components and WMO constituents, with naphthalene and octane serving as model components. Significant changes in molecular electrostatic maps, highest occupied molecular orbital and lowest unoccupied molecular orbital (HOMO-LUMO) distribution and energies, interaction energies, and hydrogen bonding networks were observed upon mixing DES with WMO. Notably, the interaction energy between naphthalene and DES components, such as the electrostatic interaction energies, was relatively higher for chloride (-2.19 kJ/mol). Moreover, MTPP (-1.06 kJ/mol), EGL (-1.21 kJ/mol) and chloride (-1.23 kJ/mol), revealed strong interactions, particularly from van der Waals forces, that facilitate effective contaminant removal. The HOMO-LUMO energy gap for the DES-naphthalene system was found to be 1.22 eV, indicating moderate electronic stability. These findings highlight the DES's capability to disrupt naphthalene-octane interactions, enhance naphthalene solubilization, and suggest its potential for improving the purification of WMO.

Keywords: Optimization; Recycling process; Used motor oil; Diesel fuel; Deep eutectic solvents.
Received: 24 February 2025; Revised: 11 April 2025; Accepted: 16 April 2025.
Article type: Research article.

1. Introduction

The diminishing availability of fossil fuel sources has spurred extensive exploration into alternative energy options. Prominent among these are renewable sources like solar and wind power, biofuels derived from organic materials such as corn or algae, and hydrogen fuel cells that generate energy through chemical reactions. These alternatives offer sustainable solutions, reducing reliance on finite fossil fuels and mitigating environmental impacts associated with their extraction and utilization.[1-3] An additional alternative gaining attention is the recycling of waste motor oil to produce diesel fuel. Waste oils originate from diverse sources including automotive, aviation, industrial, and marine sectors.

Typically, motor oil comprises base oils-mineral-based, synthetic, or blends, and various additives enhancing performance. Herein, base oils are usually around 80% aliphatic hydrocarbons (alkanes, cycloalkanes with 1-6 rings), 10% monoaromatic hydrocarbons and others. Moreover, additives in motor oil encompass detergents, dispersants, anti-wear agents, viscosity modifiers, antioxidants, corrosion inhibitors, foam inhibitors, pour-point depressants, and seal swell agents.[4-6] At the same time, waste motor oil (WMO) poses environmental hazards due to its metal contents and other contaminants such as phenols, polycyclic aromatic hydrocarbons (PAHs) and others. Approximately 45 million tons of waste oil are generated annually, with only 40% collected and disposed of, and 8% recycled into valuable products like new lubricants, diesel and others.[5-10] Efforts have intensified in recent years to recycle and reuse WMO, aiming to reduce petroleum consumption, protect the environment from hazardous chemicals, and lower greenhouse gas emissions. Various technologies are employed

[1] *Department of Transport and Mechanical Engineering, M. Kozybayev North Kazakhstan University, Petropavlovsk, 150000, Kazakhstan*
[2] *Department of Nuclear Physics, New Materials, and Technologies, L.N. Gumilyov Eurasion National University, Astana, 010008, Kazakhstan*
**Email:* abdirashevomirzak@gmail.com (O. Abdirashev); 940519400251@enu.kz (B. Satanova)

to convert WMO into diesel fuel. Recycled oil undergoes processes to remove impurities and partially restore its performance, though the efficacy of these processes may vary, impacting the quality of the reused oil. Removing impurities from WMO involves several methods, like distillation, hydrotreating, filtration, solvent extraction, acid-clay treatment, centrifugation, adsorption with activated carbon, and membrane filtration.[9-13] These techniques, often used in combination, aim to produce high-quality base oils suitable for lubricants while minimizing waste and environmental impact.

A promising approach in WMO re-refining involves deep eutectic solvents (DES). These solvents, composed of a quaternary ammonium salt and a hydrogen bond donor, form a eutectic mixture with a low melting point. DESs have been widely studied for the absorption of hydrogen disulfide from natural gas and oil, the absorption of carbon dioxide from post-combustion carbon capture processes, the purification of biodiesel from glycerol, and the recovery of lithium/cobalt from lithium-ion batteries, among others.[12-14]

Table 1 provides an overview of key studies related to WMO purification, summarizing methods, findings, and their relevance.[15-21] The studies highlight a variety of approaches, including acid-clay treatment, supercritical fluid extraction, pyrolysis, and the use of DES. These works demonstrate the effectiveness of DES and other innovative techniques in improving oil quality for diesel production.

DES efficiently dissolves impurities like heavy metals and oxidation products from WMO, offering an environmentally friendly, low-energy method for high-quality base oil recovery. This innovative technique aligns with the growing emphasis on sustainable practices in lubricant recycling. However, molecular-level comparison of traditional methyl ether ketone versus phosphor-based DES for the purification of WMO from PAHs is scarce.[22-28] In this study, naphthalene was selected as a representative PAH commonly found in WMO to model the extraction behavior of DES. This simplification enables a focused investigation of the DES–pollutant interaction mechanism. Future studies will expand the model to include additional WMO components for a more comprehensive evaluation of DES performance.

The objective of this study is to utilize DESs as an innovative and sustainable alternative for extracting impurities from WMO, transforming it into distilled or purified oil. In comparison with traditional solvents such as methyl t-butyl ether (MTBE), DESs offer significant advantages, including lower toxicity, environmental compatibility, and high extraction efficiency. To achieve a detailed understanding of the purification process, we employ a combination of density functional theory (DFT) calculations using the B3LYP functional and classical all-atom molecular dynamics (MD) simulations with the GROMOS force field. These computational approaches provide molecular-level insights into the interactions between DES and key impurities like naphthalene, highlighting the superior performance of DES in removing contaminants. The novelty of this work lies in demonstrating the dual advantages of DES for both efficient impurity extraction and environmental sustainability, setting the stage for greener solutions in WMO recycling.

In this regard, we will describe the methodology of theoretical model design, DFT calculation, classical all-atom MD simulation, and then quantum chemical and molecular structural properties for understanding the purification process of WMO from impurity.

2. Methodology

2.1 Designed systems

For our study, we chose a theoretical representation of DES using methyltriphenylphosphonium chloride (MTPPCl) and ethylene glycol (EGL) in a 1:4 ratio. As a traditional solvent for recycling WMO, we selected MTBE. In our simulations, we modeled PAHs like naphthalene as impurity in WMO, while normal octane represented motor oil components.

Table 1: List of works conducted to purify WMO into diesel.

Authors	Methods	Key findings
Troter *et al.*[15] (2016)	Review on DES Application	An extensive review on the application of DES in biodiesel purification, highlighting its effectiveness.
Smith *et al.*[16] (2016)	Acid-clay treatment	Achieved significant removal of contaminants, improving oil quality for diesel production.
Naik *et al.*[17] (2018)	Phosphorus-based DESs	Reported that phosphorus-based DESs had greater selectivity in removing PAHs.
Shah *et al.*[18] (2019)	DES	A combination of tetrabutylammonium chloride, polyethylene glycol, and ferric chloride showed high efficiency in removing sulfur compounds from fuel.
Al-Marzouqi *et al.*[19] (2019)	Supercritical fluid extraction	Demonstrated high efficiency in extracting usable hydrocarbons from WMO.
Patel *et al.*[20] (2020)	Pyrolysis	Converted WMO into biofuel with a yield of over 80%, highlighting the potential for renewable diesel.
Rakhman *et al.*[21] (2024)	Filtration and chemical treatment	Combined filtration with chemical additives to enhance purification, resulting in a cleaner end product suitable for diesel engines.

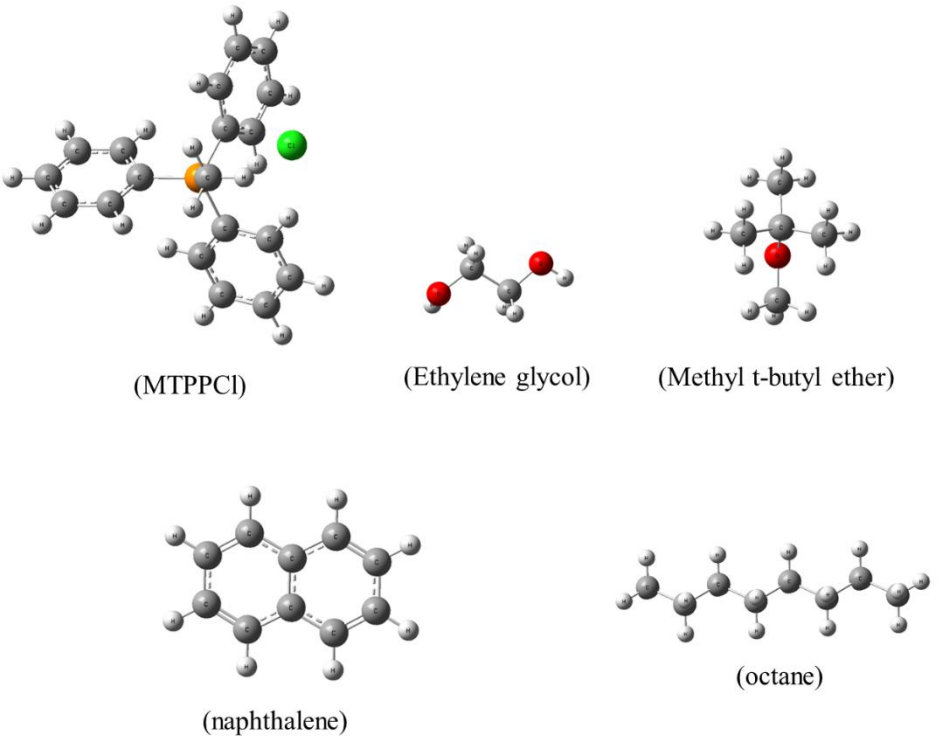

Fig. 1: 3D structure of DES, traditional solvent, and WMO components.

Fig. 1 illustrates the specific structures of the DES, traditional solvent, PAHs, and motor oil component used in our computational model for WMO recycling, which we studied through DFT calculations and classical all-atom MD simulations. WMO is a complex mixture containing a variety of contaminants, including heavy metals, PAHs, volatile organic compounds (VOCs), chlorinated solvents, and additive breakdown products. Among these, PAHs are particularly concerning due to their carcinogenic nature and environmental persistence. Naphthalene, a common PAH, was chosen for this study as it serves as a model compound for examining the behavior and removal of hazardous organic contaminants. Its prevalence in WMO, toxicological significance, and reactivity with DES make it an ideal candidate for evaluating the effectiveness of recycling strategies and understanding broader implications of oil contamination management.

The selection of a 1:4 molar ratio of MTPPCl to EGL for the DES was based on both preliminary computational screening and guidance from previous literature.[25-28] This specific ratio was found to promote stronger and more extensive hydrogen bonding networks between the hydrogen bond donor (EGL) and the hydrogen bond acceptor (MTPPCl), leading to improved stability and lower viscosity of the DES mixture. Such characteristics are particularly beneficial for facilitating pollutant solvation and transport, which are essential for efficient extraction processes. Moreover, the 1:4 ratio resulted in favorable interaction energies between DES components and target compounds like naphthalene, indicating enhanced compatibility and solvation potential. These findings support the use of this ratio as an optimal formulation for the intended waste oil purification application.

Table 2 outlines the classical all-atom MD systems designed to study the interactions between naphthalene, DES components, and WMO under various conditions. Systems 2, 3, and 4 represent DES systems with a 1:4 molar ratio of MTPPCl to EGL. System 2 includes DES alone to evaluate its intrinsic properties, while Systems 3 and 4 incorporate naphthalene and octane in 1:1000 and 5:1000 contamination ratios, respectively, to simulate real-world WMO contamination scenarios. System 1 contains only naphthalene and octane as a baseline for comparison. System5 includes MTBE, a traditional solvent, with naphthalene and octane for benchmarking the DES performance. This comprehensive

Table 2: Classical all-atom MD systems designed in this work.

No.	MTPPCl	EGL	MTBE	Naphthalene	Octane	Box size (nm^3)	Number of atoms
1	-	-	-	5	1000	6.42×6.42×6.42	26090
2	200	800	-	-	-	5.45×5.45×5.45	15800
3	200	800	-	1	1000	6.91×6.91×6.91	41818
4	200	800	-	5	1000	6.95×6.95×6.95	41890
5	-	-	800	5	1000	7.42×7.42×7.42	40490

setup enables a detailed analysis of the DES's efficacy in contaminant removal and highlights its potential advantages over conventional solvents.

2.2 DFT calculations

We employed GAUSSIAN09 and GausView for DFT calculations to optimize molecular structures, analyze molecular orbital densities, generate molecular electrostatic potential maps, determine bond lengths,[29,30] and calculate optimized energies. The focus of our study was on MTPPCl/EGL-based DESs for the purification of WMO. We optimized the electronic ground state geometries for MTPPCl, EGL, and their mixture as DESs, as well as for the DES combined with naphthalene and octane in the gas phase. These optimizations were performed using DFT with the B3LYP functional, incorporating dispersion correction, and a 6-311++G(d,p) basis set.[31,32] Additionally, we selected MTBE as a traditional solvent for comparison in the WMO purification process. We optimized the electronic ground state geometries for MTBE alone and in combination with naphthalene and octane in the gas phase using the same DFT method (Fig. 1). To ensure the accuracy of our results, we confirmed that all stationary points were true minima on their respective potential energy surfaces through analytical calculation of the second energy derivatives. This comprehensive computational analysis provides insights into the molecular interactions and stability of the DESs and traditional solvents in the context of WMO purification.

2.3 Classical all-atom MD simulations

The segment model in Fig. 1 represents the DES using MTPPCl and EGL. We constructed a model of WMO using octane with PAHs (naphthalene) as impurities. Lennard-Jones parameters were sourced from the GROMOS force field, while force field parameters (angles, dihedrals, bonds, partial charges) and coordinates for functional groups (Fig. 1) were obtained from the ATB database.[33,34] We then created representative sections of DES systems for MD simulations, with and without WMO components.

After initializing the simulation boxes, we optimized configurations at 298 K and 1 bar pressure over 0.1 ns using the steepest descent approach for energy minimization. Subsequently, we conducted NPT and NVT equilibrations for 1 ns each at 298 K and 1 bar pressure, resulting in an equilibrated box size of 10 × 10 × 10 nm³. MD simulations were performed under the NVT ensemble for 10 ns at 298 K. During the simulation, all bonds were constrained using the linear constraint solver algorithm, with a 1.0 nm cut-off for coulombic short-range interactions and Lennard-Jones interactions. Long-range interactions were computed via Particle Mesh Ewald summation with fourth-order interpolation and a 0.16 nm grid spacing. Temperature control utilized the V-rescale technique, and pressure was maintained using Berendsen pressure coupling. Periodic boundary conditions were applied in all directions.[35-37] The GROMACS software was employed for all-atom MD simulations, and visual molecular dynamics (VMD) was utilized for box visualization.[38]

To ensure the reliability of the simulation setup, the densities of all systems were calculated after equilibration and compared with available experimental values. For system 1, consisting of octane and a small amount of naphthalene, the computed density was approximately 714 kg/m³, which is in good agreement with the experimental value of 703 kg/m³. System 2, which represents the pure DES composed of MTPPCl and EGL, exhibited a density of 1127 kg/m³, closely matching the reported experimental density of 1132 kg/m³. For Systems 3 to 5, representing DES mixed with WMO components at various compositions, the calculated density was around 943 kg/m³, compared to the experimental value of 950 kg/m³.[15-18] The close agreement between the simulated and experimental densities demonstrates the accuracy of the force field parameters and the overall validity of the computational models employed in this study.

Although the current study is primarily based on DFT and classical all-atom MD simulations, it provides valuable insights into the molecular interactions and extraction potential of the studied DES systems. However, we recognize the necessity of validating the computational predictions with experimental evidence. Our research team is currently preparing to conduct complementary experimental studies to evaluate the effectiveness of MTPPCl-EGL-based DESs in removing aromatic contaminants, such as naphthalene, from real WMO samples. These future experimental efforts will serve to validate the simulation results and further establish the practical applicability of the designed DES systems for sustainable waste oil purification.

3. Results and discussion

3.1 DFT calculation results and discussions

In this study, we employed DFT using the B3LYP functional to explore the extraction efficiency of naphthalene from octane using a novel DES composed of MTPPCl and EGL. This section discusses the results, with a particular focus on the optimized molecular structures, electrostatic potential maps, and Highest occupied molecular orbital and Lowest unoccupied molecular orbital (HOMO-LUMO) energy levels, which provide insights into the interaction mechanisms between the DES and the naphthalene-octane mixture.

Fig. 2a illustrates the optimized molecular structure of the octane-naphthalene-DES system. The figure reveals that naphthalene is predominantly positioned near the chloride and EGL moieties of the DES, suggesting strong interactions between these components. This proximity indicates that the chloride ions and EGL play a crucial role in stabilizing the naphthalene molecule within the DES matrix. The preferential localization of naphthalene near chloride ions and EGL in the DES system can be attributed to a balance of electrostatic and van der Waals interactions. The chloride ions attract naphthalene's electron-rich aromatic rings through

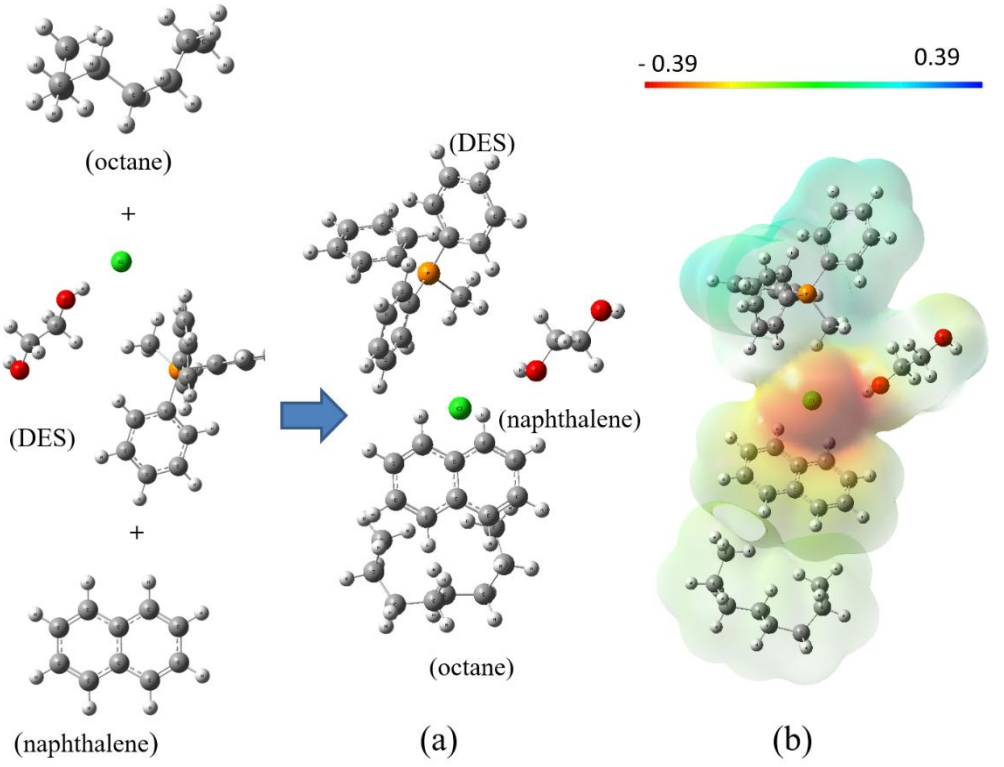

Fig. 2: (a) Optimized structures, (b) molecular electrostatic maps for MTPPCl and EGL-based DES and DES + naphthalene + octane. Color key: white: hydrogen; grey: carbon; blue: nitrogen; oxygen: red; yellow: sulfur; and green: chloride.

electrostatic forces, while van der Waals interactions between the hydrophobic naphthalene and EGL provide additional stabilization (as can be noted in subsection 3.2). This interplay highlights the DES system's efficiency in targeting hydrophobic and aromatic contaminants for removal. On the other hand, octane is located near the naphthalene molecule, suggesting a weaker interaction with the DES. The relative positioning of these molecules suggests that DES is more effective in targeting polar or aromatic compounds like naphthalene, compared to non-polar hydrocarbons like octane.

The molecular electrostatic potential map presented in Fig. 2b further supports this observation. The molecular electrostatic potential map shows significant charge delocalization around the chloride and oxygen atoms of the DES, which correlates with the regions of high electron density. This delocalization is indicative of strong electrostatic interactions between the DES and naphthalene, which are likely responsible for the efficient extraction of naphthalene from the octane-naphthalene mixture. The electrostatic potential map highlights the role of chloride and oxygen atoms in creating favorable conditions for naphthalene to interact with the DES, thereby facilitating its extraction from octane.

Fig. 3 provides the HOMO and LUMO orbitals for the octane-naphthalene-DES system. The analysis reveals that the HOMO is primarily distributed around the naphthalene and chloride atoms, indicating that the HOMO is influenced by the naphthalene-DES interaction. In contrast, the LUMO is localized around the MTPP moiety of the DES, suggesting that the LUMO is more associated with the DES's structural backbone. The energy gap between HOMO (-3.80 eV) and LUMO (-2.58 eV) indicates a moderate level of electronic stability, which is crucial for maintaining the integrity of the DES during the extraction process. The localization of the HOMO and LUMO orbitals around different parts of the DES-naphthalene system underlines the selective interaction mechanisms that DES can exploit to efficiently separate aromatic compounds from hydrocarbon mixtures.

For comparative analysis, the extraction of naphthalene from octane was also investigated using a traditional solvent, MTBE. The optimized structures and MEP maps are depicted in Fig. 4, respectively. The structural analysis (Fig. 4a) shows that naphthalene is situated near the ether groups of MTBE, while octane remains in close proximity to naphthalene, similar to the DES system. However, the molecular electrostatic potential map (Fig. 4b) reveals a different charge distribution, with significant delocalization around both the naphthalene and the ether groups, indicating that MTBE interacts with naphthalene primarily through van der Waals forces. The HOMO-LUMO analysis for the MTBE-Naphthalene-Octane system, shown in Fig. 5, demonstrates that the HOMO and LUMO orbitals are both localized near the naphthalene molecule. The HOMO energy is -5.93 eV and the LUMO energy is -1.22 eV. Moreover, the distribution of the HOMO and LUMO orbitals is primarily concentrated around the naphthalene molecule. In contrast, in Fig. 4, the HOMO is distributed around both naphthalene and the chloride ion, while the LUMO is localized around the MTPPCl component of the DES.

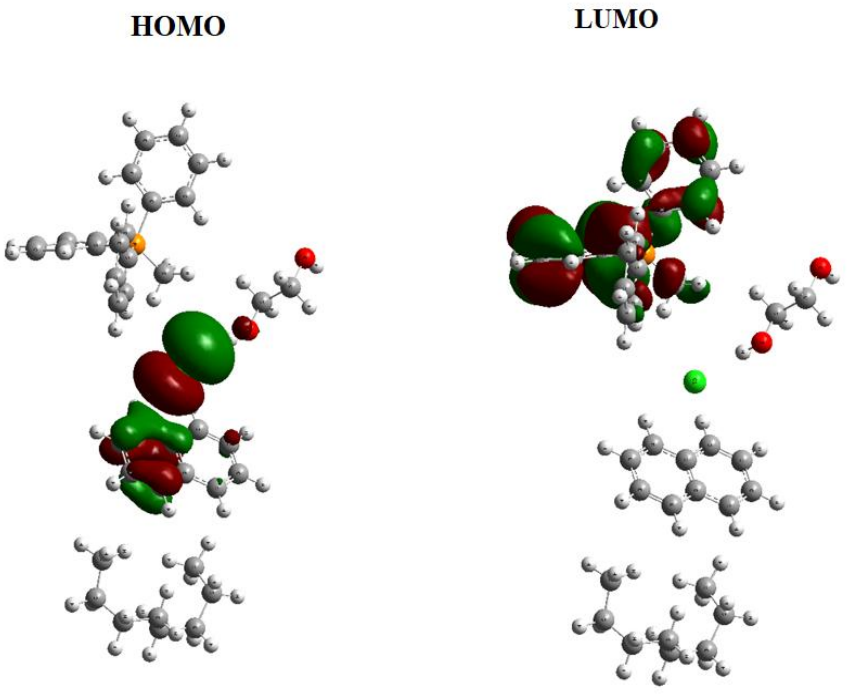

Fig. 3: Molecular orbital density for optimized structures of naphthalene, octane, DES, and DES + naphthalene + octane. The green and red isosurfaces illustrate the spatial distribution and phase of the LUMO, corresponding to positive and negative orbital lobes, respectively.

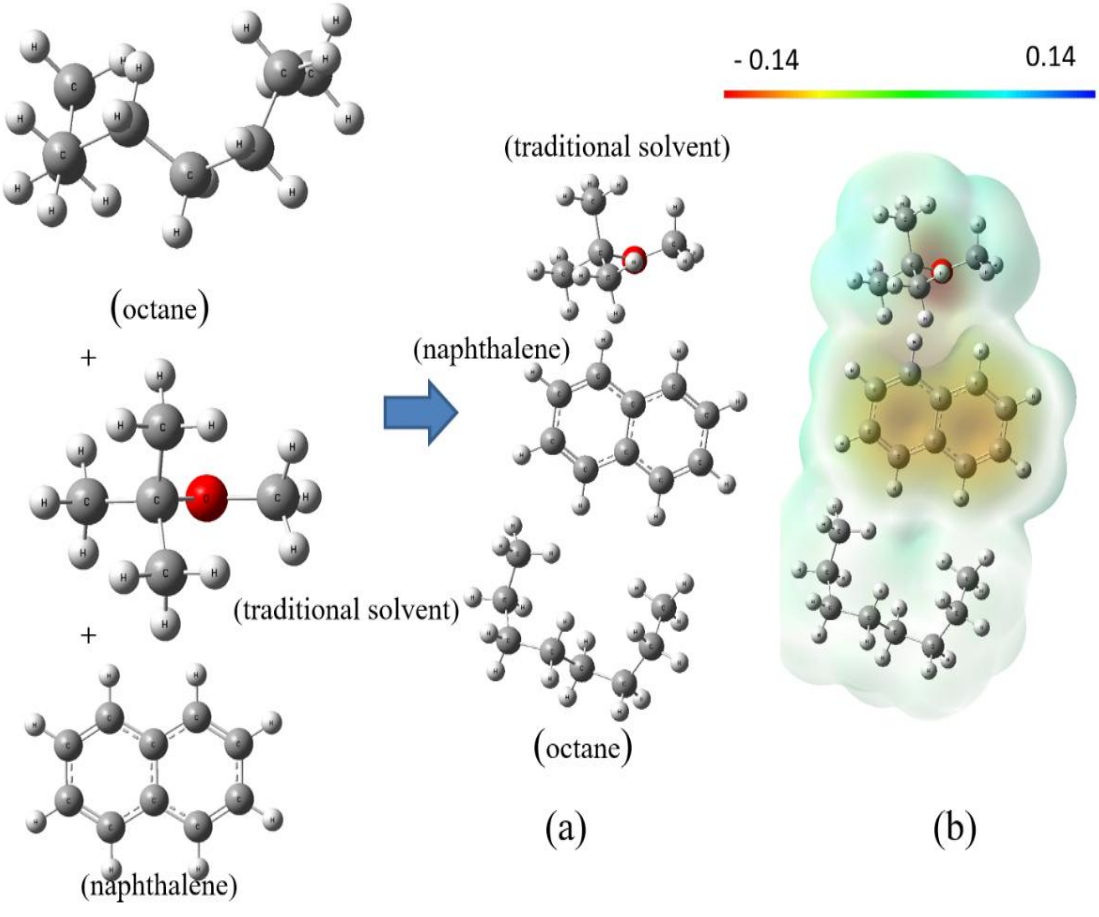

Fig. 4: (a) Optimized structures, (b) molecular electrostatic maps for MTBE-based traditional solvent and traditional solvent + naphthalene + octane. Color key: white: hydrogen; grey: carbon; blue: nitrogen; oxygen: red; yellow: sulfur; and green: chloride.

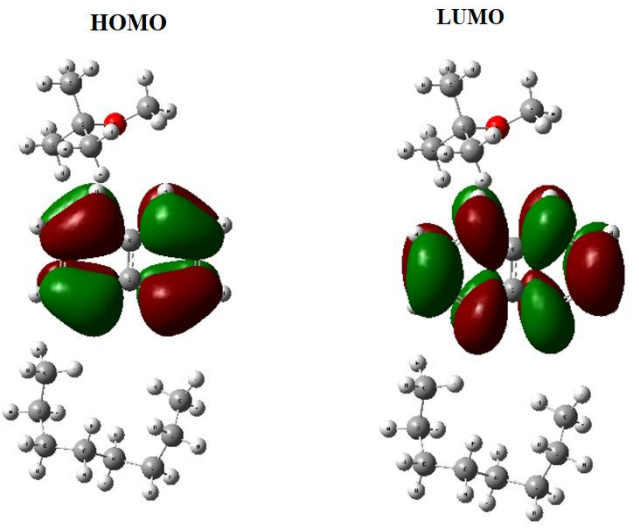

Fig. 5: Orbital density for optimized structures of naphthalene, octane, traditional solvent, and traditional solvent + naphthalene + octane. The green and red isosurfaces illustrate the spatial distribution and phase of the LUMO, corresponding to positive and negative orbital lobes, respectively.

3.2 Classical all-atom MD simulation results and discussions

In this study, we employed classical all-atom MD simulations to investigate the intermolecular interactions within a DES composed of MTPPCl and EGL. The focus of our research was on the efficacy of this DES in the removal of naphthalene, a model component representing WMO, in the presence of octane. Our simulations provide detailed atomistic insights into the structural and interaction dynamics of the DES and its capability to selectively target and remove naphthalene from a mixture simulating WMO. The ratio of MTPPCl to EGL in the DES formulation was chosen as 1:4 (molar basis) based on prior studies demonstrating the superior efficacy of this composition in impurity removal[21, 23, 39-41]. This ratio ensures an optimal hydrogen bonding network between the DES components, enhancing its ability to solubilize and separate nonpolar impurities such as naphthalene.

Figs. 6a and 6b present a snapshot of the classical all-atom MD simulations of the DES alone. The structural arrangement of the DES components, MTPPCl, and EGL, demonstrates a complex network of hydrogen bonds and ionic interactions. The chloride anions interact strongly with the hydroxyl groups of EGL, stabilizing the DES matrix. The presence of the bulky MTPP cations further contributes to the overall stability through van der Waals interactions and steric effects, enhancing the DES's viscosity and potential solvent capabilities.

Figs. 6c and 6d illustrate the behavior of the DES in the presence of naphthalene and octane. The snapshot reveals that naphthalene molecules are predominantly located near the DES, whereas octane molecules remain outside the DES matrix. This selective interaction is crucial for the DES's application in purifying WMO. The preferential affinity of the DES for naphthalene can be attributed to π-π stacking interactions between the aromatic rings of naphthalene and the chloride ion, ethylene glycol and phenyl groups of MTPPCl.

The MD simulations highlight that the DES forms a microenvironment conducive to encapsulating and solvating naphthalene, effectively isolating it from the surrounding octane. This selective solubility suggests that the DES can efficiently extract aromatic contaminants like naphthalene from a mixture, leaving non-aromatic hydrocarbons such as octane relatively unaffected. The ability to differentiate between aromatic and non-aromatic components is a key advantage for recycling processes, as it allows for the targeted removal of harmful or undesirable substances while preserving valuable hydrocarbons.

The findings from our MD simulations have significant implications for the recycling of WMO into diesel fuel. The selective removal of naphthalene by the DES demonstrates its potential as an effective purification agent. By extracting aromatic contaminants, the DES can help in refining WMO, reducing the presence of harmful PAHs and improving the quality of the resulting diesel fuel.

Furthermore, the atomistic-level understanding of the interaction mechanisms provides insights into optimizing the DES composition for enhanced performance. The balance between the ionic and hydrogen-bonding components can be fine-tuned to maximize the solubility and selectivity towards target contaminants. This approach can lead to the development of tailored DES formulations with specific properties suited for various recycling and purification applications.

Our classical all-atom MD simulations have elucidated the interaction dynamics of an MTPPCl and EGL-based DES with naphthalene and octane. The DES exhibits a strong affinity for naphthalene, effectively separating it from octane, demonstrating its potential for purifying WMO. These findings provide a foundation for further exploration and optimization of DES formulations, paving the way for more efficient and sustainable recycling processes in the future. To further analyze the interactions within the DES and its efficiency in removing naphthalene from WMO, we evaluated the interaction energies of the DES components before and after mixing with WMO, as summarized in Table 3. This comprehensive analysis provides insight into the structural and functional dynamics of the DES system.

In pure MTPPCl, the interaction between the MTPP cation and the chloride anion is characterized by an electrostatic energy of -2956.19 kJ/mol and a van der Waals energy of -1207.45 kJ/mol. These strong values indicate a stable ionic bond, contributing to the solid-state stability of MTPPCl. The high electrostatic interaction demonstrates the significant attraction between the oppositely charged ions, while the van der Waals contribution further stabilizes the overall structure. Upon forming the DES with EGL, notable changes in the interaction energies occur. The electrostatic interaction

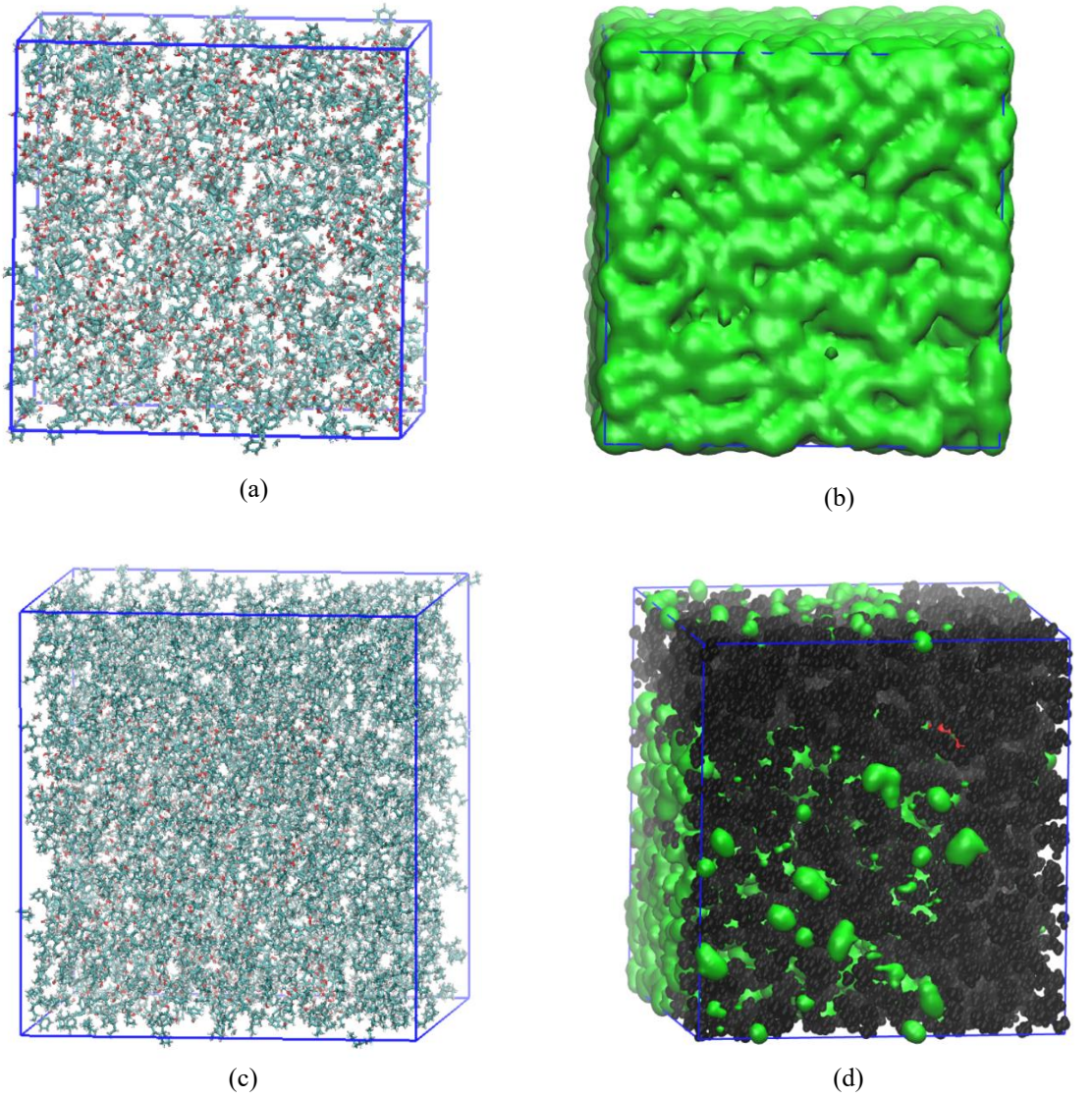

Fig. 6: Snapshot of classical all-atom MD simulations for (a) bond, (b) isosurface representation of DES, (c) bond, and (d) isosurface representation of DES in the presence of naphthalene and octane to mimic the process of purification of WMO. Color key: white: hydrogen; grey: carbon; blue: nitrogen; oxygen: red; yellow: sulfur; green: chloride; green isosurface: DES; black VDM representation: WMO.

Table 3: Interaction energy for pure MTPPCl and DES components before and after mixing with WMO.

Energy (kJ/mol)	Pure MTPPCl		DES		DES + WMO	
	Electrostatic	Van der Waals	Electrostatic	Van der Waals	Electrostatic	Van der Waals
MTPP and chloride	-2956.19	-1207.45	-2034.54	-307.14	-1956.67	-322.25
EGL and MTPP	-	-	-754.05	-4356.41	-723.12	-4319.37
EGL and chloride	-	-	-13351.10	6771.4	-13430.50	6820.85

between MTPP and chloride decreases to -2034.54 kJ/mol, while the van der Waals energy reduces to -307.14 kJ/mol. This reduction reflects the disruption of direct ionic interactions between MTPP and chloride due to the introduction of EGL, which actively participates in extensive hydrogen bonding and van der Waals interactions with both components.

The role of EGL in stabilizing the DES structure is evident from its interactions with MTPP and chloride. The interaction energy between EGL and MTPP is -754.05 kJ/mol (electrostatic) and -4356.41 kJ/mol (van der Waals). These values highlight the contribution of EGL in forming a robust

network of hydrogen bonds and van der Waals forces. The interaction between EGL and chloride is even more significant, with an electrostatic energy of -13351.10 kJ/mol and a van der Waals energy of 6771.4 kJ/mol, underscoring the strong hydrogen bonding network that plays a crucial role in maintaining DES stability and functionality.

When the DES is mixed with WMO, further changes in interaction energies are observed. The interaction energy between MTPP and chloride slightly increases to -1956.67 kJ/mol (electrostatic) and -322.25 kJ/mol (van der Waals), indicating a marginally enhanced interaction. This could result from the rearrangement of DES components to incorporate WMO constituents such as naphthalene and octane. Similarly, the interaction energy between EGL and MTPP decreases slightly to -723.12 kJ/mol (electrostatic) and -4319.37 kJ/mol (van der Waals), suggesting that part of EGL's interaction potential is redirected to interact with WMO components.

The most notable change is observed in the interaction energy between EGL and chloride, which increases to -13430.50 kJ/mol (electrostatic) and 6820.85 kJ/mol (van der Waals). This enhancement indicates stronger interactions, likely due to the DES restructuring to solubilize naphthalene. MD simulations support this observation, showing that naphthalene tends to localize near the DES matrix, where it forms selective interactions. The interaction energy analysis demonstrates the DES's stability and selective affinity for aromatic compounds like naphthalene. The strong hydrogen bonding network between EGL and chloride ensures the DES's structural integrity, even in the presence of WMO. The selective solubilization of naphthalene, driven by π-π stacking with MTPP and hydrogen bonding with EGL, highlights the DES's efficiency in removing aromatic contaminants while leaving non-aromatic hydrocarbons like octane relatively unaffected.

These findings underscore the potential of the MTPPCl and EGL-based DES in WMO purification processes. The ability to selectively target and remove naphthalene enhances the quality of recycled motor oil, making this DES a promising candidate for sustainable waste management and resource recovery applications. Future studies can optimize DES formulations by exploring alternative hydrogen bond donors and acceptors, as well as studying the effects of varying operational conditions like temperature, pressure, and concentration. Overall, the interaction energy data, coupled with MD simulations, provide a comprehensive understanding of the DES's behavior and efficacy in WMO purification. These insights pave the way for developing advanced DES formulations tailored to specific contaminants, contributing to sustainable and efficient purification technologies.

To gain further insights into the structural dynamics and stability of the DES in the presence of WMO, we examined the number of hydrogen bonds between the DES components before and after mixing with WMO. Table 4 summarizes the hydrogen bond counts for EGL with MTPP and chloride in both scenarios. In the pure DES, the formation of hydrogen bonds is a crucial factor contributing to its stability and functionality. The data show that there are 86 hydrogen bonds between EGL and MTPP, indicating a significant interaction that helps stabilize the DES matrix. The presence of 682 hydrogen bonds between EGL and chloride further underscores the critical role of hydrogen bonding in maintaining the structural integrity and solvation properties of the DES. These strong interactions facilitate the DES's ability to solvate and interact with various molecules, including potential contaminants in WMO.

Table 4: Number of hydrogen bonds between DES components before and after mixing with WMO.

Number of H-bonds	DES	DES + WMO
EGL and MTPP	86	81
EGL and chloride	682	471

Upon mixing the DES with WMO, the number of hydrogen bonds changes, reflecting the interaction dynamics with the new components. The hydrogen bonds between EGL and MTPP decrease slightly to 81. This minor reduction suggests that some of the hydrogen bonding capacity of EGL is now being utilized to interact with the WMO components, particularly naphthalene. The most significant change is observed in the hydrogen bonds between EGL and chloride, which decrease to 471. This reduction indicates a substantial reorganization of the hydrogen bonding network within the DES to accommodate the presence of WMO. The lower number of hydrogen bonds suggests that EGL is engaging in interactions with naphthalene and potentially other components of the WMO, thereby reducing its capacity to form hydrogen bonds with chloride.

The reduction in hydrogen bonds between EGL and both MTPP and chloride upon mixing with WMO highlights the adaptability and flexibility of the DES structure. The ability to reorganize its hydrogen bonding network is crucial for the DES to effectively interact with and solubilize contaminants such as naphthalene. The decrease in hydrogen bonds between EGL and chloride, in particular, suggests that EGL is strongly interacting with naphthalene, as supported by the MD simulation snapshots. This interaction likely involves the formation of hydrogen bonds and other non-covalent interactions, facilitating the solubilization of naphthalene within the DES matrix.

The ability of the DES to adjust its hydrogen bonding network to accommodate and solubilize naphthalene underscores its effectiveness in removing aromatic contaminants from WMO. The selective reduction in hydrogen bonds with chloride, while maintaining a stable interaction network, indicates that the DES can efficiently target and solubilize specific contaminants without compromising its overall structural integrity. This selective interaction is crucial for the practical application of the DES in recycling processes. By effectively solubilizing and removing naphthalene, the DES can improve the quality of the

Table 5: Interaction energy for naphthalene with octane and DES components.

Energy (kJ/mol)	Pure WMO (5:1000 ratio of naphthalene to octane)		WMO (1:1000 ratio of naphthalene to octane) with DES		WMO (5:1000 ratio of naphthalene to octane) with DES	
	Electrostatic	Van der waals	Electrostatic	Van der waals	Electrostatic	Van der waals
Naphthalene and Octane	0.12	-4.52	0.02	-0.74	0.097	-2.40
Naphthalene and MTPP			-0.01	-0.015	0.05	-1.06
Naphthalene and EGL			-0.005	-0.011	-0.02	-1.21
Naphthalene and chloride			-0.025	-0.14	-2.19	-1.23

recycled motor oil, reducing the presence of harmful PAHs and enhancing the performance of the resulting diesel fuel.

Understanding the dynamics of hydrogen bonding within the DES provides valuable insights for optimizing its formulation. By fine-tuning the composition and ratio of components, it is possible to enhance the DES's ability to form and reorganize hydrogen bonds, improving its efficiency in solubilizing specific contaminants. Future research could explore the impact of varying the concentration of WMO components, temperature, and pressure on the hydrogen bonding dynamics. Additionally, investigating alternative hydrogen bond donors and acceptors could lead to the development of DESs with tailored properties for specific applications in waste management and resource recovery.

The analysis of hydrogen bonds between DES components before and after mixing with WMO provides a deeper understanding of the interaction dynamics and structural adaptability of the DES. The reduction in hydrogen bonds between EGL and chloride, in particular, highlights the DES's ability to selectively interact with and solubilize naphthalene, demonstrating its potential for efficient purification of WMO. These findings offer a foundation for further optimization and application of DESs in various purification and recycling processes, contributing to more sustainable and efficient solutions in waste management and resource recovery.

The interaction energies summarized in Table 5 provide valuable insights into the dynamics between naphthalene, a model aromatic contaminant, and both the WMO and DES components. These energies reveal how the DES facilitates the selective separation of naphthalene from octane and highlights its efficacy as a purification medium.

In the pure WMO system with a 5:1000 ratio of naphthalene to octane, the interaction energy between naphthalene and octane is dominated by weak van der Waals forces, yielding a value of -4.52 kJ/mol. The electrostatic contribution is minimal, at 0.12 kJ/mol, due to the non-polar nature of both molecules. These weak interactions indicate that naphthalene can be relatively easily separated from octane, as their affinity for each other is low.

When DES is introduced into the WMO system at a 1:1000 ratio of naphthalene to octane, the interaction energy between naphthalene and octane decreases significantly to -0.74 kJ/mol. This reduction indicates that the DES disrupts the interactions between naphthalene and octane by preferentially interacting with naphthalene. Specifically, the interaction energy between naphthalene and MTPP is -0.01 kJ/mol electrostatic and -0.015 kJ/mol van der Waals, suggesting weak π-π stacking interactions between the aromatic ring of naphthalene and the phenyl groups of MTPP. Similarly, the interaction energy between naphthalene and EGL is -0.011 kJ/mol van der Waals, reflecting its role as a hydrogen bond donor interacting with naphthalene's π-electrons. The interaction energy between naphthalene and chloride ions is more substantial, at -0.14 kJ/mol van der Waals, indicating a significant electrostatic attraction between chloride and the aromatic ring of naphthalene. These findings align with the results from DFT simulations, which show that naphthalene preferentially localizes near chloride ions and EGL due to a balance of electrostatic and van der Waals forces.

At a higher concentration of naphthalene in WMO (5:1000 ratio), the interaction energy trends remain consistent, but the magnitudes change. The interaction energy between naphthalene and octane decreases further to -2.40 kJ/mol van der Waals, reflecting the increasing disruption of naphthalene-octane interactions by the DES. The interaction energy between naphthalene and MTPP becomes more pronounced, at -1.06 kJ/mol van der Waals, indicating enhanced π-π stacking interactions due to the higher availability of MTPP. Similarly, the interaction energy between naphthalene and EGL increases to -1.21 kJ/mol van der Waals, highlighting improved stabilization of naphthalene by EGL. The electrostatic interaction energy between naphthalene and chloride ions increases substantially to -2.19 kJ/mol, demonstrating a strong attraction between the electron-rich naphthalene and chloride ions within the DES matrix.

These results provide a clear understanding of the DES's ability to effectively solubilize naphthalene. The significant reduction in the interaction energy between naphthalene and octane in the presence of DES demonstrates its capability to facilitate the separation of naphthalene from WMO. The preferential localization of naphthalene near chloride ions and EGL is driven by a combination of electrostatic and van der

Waals interactions. This interplay underscores the DES system's efficiency in targeting hydrophobic and aromatic contaminants for removal.

The interaction energy analysis highlights the potential of DES for purification applications, particularly in separating naphthalene from WMO. The strong interactions between naphthalene and the DES components, especially at higher concentrations, demonstrate the DES's capacity to disrupt naphthalene-octane interactions and enhance the solubilization of naphthalene. Further research is recommended to explore the effects of varying operational parameters, such as temperature and pressure, on these interaction dynamics. Additionally, examining the recyclability and regeneration of DESs can provide insights into their long-term viability and economic feasibility for large-scale applications.

The molecular-level interactions between DES components and naphthalene provide critical insights into their effectiveness in removing hydrophobic and aromatic contaminants. Our classical all-atom MD simulations reveal that naphthalene preferentially localizes near chloride ions and ethylene glycol molecules within the DES system. This behavior arises from a delicate balance of electrostatic and van der Waals interactions.

The chloride ions, with their high charge density, attract the electron-rich aromatic rings of naphthalene, resulting in significant electrostatic interactions. Simultaneously, van der Waals interactions between naphthalene and the hydrophobic regions of ethylene glycol contribute additional stabilization. This interplay of forces not only enhances the solubility of naphthalene in the DES matrix but also underscores the system's efficiency in targeting hydrophobic and aromatic contaminants. These findings highlight the superiority of DES over traditional solvents, as the latter often lack the dual capability of electrostatic and hydrophobic interactions. By elucidating these molecular-level mechanisms, this study advances the understanding of DES as a sustainable and selective alternative for the removal of PAHs and similar impurities from waste streams. These findings lay the groundwork for further optimization and application of DESs in various purification and recycling processes. By leveraging the unique properties of DESs, it is possible to develop sustainable and efficient solutions for waste management and resource recovery, contributing to a cleaner and more sustainable future.

To further evaluate the efficiency of the DES in removing naphthalene from WMO, the interaction energies of naphthalene with octane and DES components were compared against those with a traditional solvent. Table 6 presents the interaction energies in terms of electrostatic and van der Waals contributions for both systems.

In the DES + WMO system at a 5:1000 naphthalene-to-octane ratio, the interaction energy between naphthalene and octane shows a significant reduction, with the van der Waals contribution decreasing to -2.40 kJ/mol and a minimal electrostatic contribution of 0.097 kJ/mol. This reduction highlights the DES's ability to disrupt naphthalene-octane interactions, facilitating the preferential solubilization of naphthalene within the DES matrix. This trend aligns with the findings from DFT simulations, where the DES components exhibited strong interactions with naphthalene, effectively reducing its affinity for octane.

The interaction energy between naphthalene and MTPP is characterized by a van der Waals contribution of -1.06 kJ/mol, indicating moderate π-π stacking interactions between the aromatic ring of naphthalene and the phenyl groups of MTPP. These interactions are essential for stabilizing naphthalene within the DES matrix and preventing its aggregation. For the naphthalene-EGL pair, the van der Waals interaction energy is -1.21 kJ/mol, slightly stronger than the interaction with MTPP. This can be attributed to effective hydrogen bonding between EGL, a hydrogen bond donor, and the π-electrons of naphthalene. The electrostatic interaction with EGL is minimal (-0.02 kJ/mol), further confirming the dominance of non-covalent forces in stabilizing naphthalene.

Chloride ions, although not directly interacting strongly with naphthalene (van der Waals energy of -1.23 kJ/mol), play a critical role in the overall stability of the DES. The strong electrostatic interaction between naphthalene and chloride (-2.19 kJ/mol) indicates a notable attraction, supporting the idea that chloride ions contribute indirectly to the solubilization of naphthalene by maintaining the structural integrity of the DES network. In contrast, the traditional solvent system with MTBE shows weaker performance in disrupting naphthalene-

Table 6: Interaction energy for naphthalene with octane, DES components and traditional solvent.

Energy (kJ/mol)	DES + WMO (5:1000)		Traditional solvent + WMO (5:1000)	
	Electrostatic	Van der waals	Electrostatic	Van der waals
Naphthalene and Octane	0.097	-2.40	0.07	-3.28
Naphthalene and MTPP	0.05	-1.06	-	-
Naphthalene and EGL	-0.02	-1.21	-	-
Naphthalene and chloride	-2.19	-1.23	-	-
Naphthalene and MTBE	-	-	0.10	-1.27

octane interactions. The interaction energy between naphthalene and octane in the traditional solvent system is reduced to -3.28 kJ/mol (van der Waals), which is less effective than the reduction observed with DES. The naphthalene-MTBE interaction energy of -1.27 kJ/mol (van der Waals) is slightly stronger than the interactions between naphthalene and EGL or MTPP in the DES system. However, the traditional solvent lacks the synergy of electrostatic and non-covalent interactions provided by the DES components, limiting its overall efficacy in solubilizing naphthalene.

This comparative analysis reveals the superior performance of DES over traditional solvents for removing aromatic contaminants like naphthalene from WMO. The lower interaction energy between naphthalene and octane in the DES system (-2.40 kJ/mol) compared to the traditional solvent system (-3.28 kJ/mol) underscores the DES's efficiency in disrupting weak van der Waals forces. Furthermore, the moderate to strong interactions between naphthalene and DES components (MTPP and EGL), coupled with the indirect stabilization provided by chloride ions, enhance the solubilization and stabilization of naphthalene within the DES matrix. These findings align with the DFT results, which emphasize the DES's ability to establish hydrogen bonding and π-π stacking interactions. This interplay between electrostatic and non-covalent forces explains the DES's superior efficacy in breaking down naphthalene-octane interactions and stabilizing naphthalene within its structure.

The enhanced performance of DES in removing naphthalene from WMO has significant implications for sustainable waste management and resource recovery. The ability of DES to disrupt naphthalene-octane interactions while stabilizing naphthalene within its matrix suggests its potential for broader applications in purifying WMO and producing higher-quality
recycled diesel fuel.

Future work should focus on optimizing DES formulations to improve their performance across a wider range of contaminants. Exploring alternative hydrogen bond donors and acceptors and varying the ratios of DES components could lead to tailored formulations for specific applications. Additionally, studies on the recyclability and regeneration of DESs will be crucial for assessing their economic feasibility and environmental sustainability. This analysis demonstrates that DES, with its unique combination of electrostatic and van der Waals interactions, offers a more efficient and sustainable solution than traditional solvents for removing aromatic contaminants from WMO. Traditional solvents, such as MTBE, have been widely used for contaminant removal due to their ability to dissolve hydrocarbons effectively. However, their use raises concerns regarding toxicity, environmental pollution, and limited reusability. DES offers a promising alternative, combining high efficiency with sustainability. DES are composed of biodegradable and non-toxic components, which significantly reduce the environmental footprint. Moreover, their selective interaction with contaminants like PAHs enhances their efficacy in recycling processes.

To emphasize the advantages of DES, a comparison with traditional solvents is presented in Table 7. This comparison underscores how DES outperforms conventional methods in terms of efficiency, cost, and environmental impact, reinforcing their potential for sustainable WMO recycling. While this study demonstrates the strong extraction capability of the MTPPCl-EGL DES for aromatic pollutants in WMO, practical applications also require consideration of long-term performance. Factors such as solvent degradation, recyclability, and regeneration efficiency can significantly influence the overall sustainability and cost-effectiveness of the process. These aspects were beyond the scope of the present computational investigation but will be explored in future work combining experimental and techno-economic analyses.

To provide a more comprehensive view of WMO recovery technologies, Table 8 compares the DES-based extraction method with other modern recovery techniques such as vacuum distillation, pyrolysis, and catalytic cracking. While traditional solvents like MTBE and DES were directly

Table 7: Comparison of DES vs traditional solvent for recycling of WMO.[18-22]

Property	Traditional Solvents	DES
Efficiency	Moderate, effective for hydrocarbons but limited selectivity	High, selective interaction with specific contaminants like PAHs
Cost	Relatively high due to synthesis and processing costs	Low, composed of inexpensive, readily available components
Toxicity	Toxic, poses health and environmental hazards	Non-toxic, safer for human and environmental health
Environmental impact	Significant, contributes to pollution and requires careful disposal	Minimal, biodegradable and eco-friendly
Reusability	Limited, often single-use	High, can be regenerated and reused in multiple cycles

Table 8: Analyzes the study's solvent-based approach against other modern WMO recovery methods.[40-44]

Method	Description	Key features	Comparison to DES approach
Traditional solvent Extraction (*e.g.*, MTBE)	Uses hydrocarbon solvents to dissolve impurities, followed by separation	- Established industrial process - Moderate contaminant removal efficiency - Potential solvent toxicity concerns	Directly compared in study, DES showed superior intermolecular interactions and selectivity
DES-based extraction	Employs methyltriphenylphosphonium chloride/ethylene glycol eutectic mixture	- Green chemistry approach - High naphthalene selectivity - Atomistic validation via DFT/MD	Study's focus demonstrated effective disruption of aromatic-aliphatic interactions
Vacuum distillation & hydrotreatment	Combines fractional distillation with catalytic hydrogenation	- Industry-standard for base oil production - Energy-intensive (400-500 °C) - Removes additives/metals	Not addressed, thermal vs solvent-based purification
Pyrolysis/Gasification	Thermal decomposition into syngas or pyrolysis oil	- Handles mixed plastic waste - Produces hydrocarbon feedstocks - High temperature (>700 °C)	Study focused on liquid-phase extraction rather than thermal conversion
Catalytic cracking	Zeolite-catalyzed molecular breakdown	- Direct diesel production - Requires catalyst regeneration - Handles heavy fractions	Not compared; catalytic vs solvent interaction mechanisms differ fundamentally

compared in this study, other modern methods were also considered to evaluate the strengths and weaknesses of the solvent-based approach in the broader context of WMO purification processes.

While this study provides valuable mechanistic insights into the atomistic interactions between DES components and WMO constituents, several practical considerations, including cost analysis, energy consumption, and environmental impact, remain unaddressed. For instance, although DES components like MTPPCl and ethylene glycol are generally cheaper than ionic liquids, the production costs of DES were not examined in this study. Life-cycle assessments of choline chloride-based DES show that production costs can be 15-30% higher than those of conventional solvents like methanol.[35-40] Furthermore, the scalability and economic feasibility of DES-based extraction in industrial applications would require additional cost-benefit analyses, particularly regarding solvent regeneration and recycling. Recent studies suggest that solvent regeneration can recover significant value from DES systems, such as with rGO composites, achieving 94.8% desulfurization efficiency through reuse.

In terms of energy consumption, DES extraction typically operates at ambient temperatures, offering a potential advantage over high-temperature processes like vacuum distillation, which operates at 400-500 °C. However, the study did not quantify the energy savings, and challenges such as the high viscosity of DES (often >200 cP) could lead to higher pumping energy costs compared to traditional solvents like MTBE (0.55 cP).[38-42] Additionally, no data on the energy requirements for DES-WMO phase separation post-treatment were provided.

Environmental impact considerations are also crucial. While DESs are considered "green" solvents, their ecological footprint is not fully explored in this study. For example, ChCl/urea-based DES has shown 40% higher aquatic toxicity than ethanol in life-cycle assessments. Moreover, the degradation products of spent MTPPCl-based solvents remain unaddressed, as well as the carbon footprint of DES production, which is higher than that of methanol (2.1 kg CO_2-eq/kg vs. 1.3 kg CO_2-eq/kg).[40-43] A more comprehensive life-cycle analysis comparing DES to thermal and catalytic WMO recovery methods would provide deeper insights into its environmental and economic viability. In future studies, extending atomistic models to predict the recyclability, molecular degradation thresholds, and solvent loss mechanisms of DES would be beneficial in understanding the long-term sustainability of this purification technology.[44]

4. Conclusion

This study provides a molecular-level analysis of the interactions between MTPPCl and EGL-based DES and WMO components, with a particular focus on naphthalene removal. DFT analysis revealed key insights from molecular electrostatic maps, molecular orbital distributions, and

optimized structures, showcasing the DES's structural and electronic adaptability. The electrostatic maps highlighted regions of high electron density around chloride ions and EGL, aligning with the interaction hotspots of naphthalene's aromatic rings. HOMO-LUMO analysis demonstrated a moderate energy gap of 1.22 eV for the DES-naphthalene system, indicating its electronic stability and ability to facilitate interactions. Optimized structures revealed a robust hydrogen-bonding network within the DES, further enhancing its affinity for naphthalene while disrupting its weak interactions with octane.

Classical all-atom MD simulations extended these findings, providing dynamic evidence of DES effectiveness. Interaction energy calculations showed significant van der Waals contributions between naphthalene and DES components, particularly EGL (-1.21 kJ/mol) and MTPP (-1.06 kJ/mol), while chloride ions displayed stronger electrostatic interactions with naphthalene compared to van der Waals forces. This trend, consistent with DFT results, highlights the preferential localization of naphthalene near chloride ions and EGL in the DES. The electrostatic attraction between chloride ions and naphthalene's electron-rich aromatic rings, combined with the van der Waals stabilization provided by EGL, underscores the DES's efficiency in targeting hydrophobic and aromatic contaminants for removal. Snapshots from MD simulations revealed the dynamic reorganization of the hydrogen-bonding network within the DES upon mixing with WMO. These adjustments enhance the DES's capacity to solubilize naphthalene and disrupt its weak interactions with octane, as evidenced by reduced interaction energies and altered bonding patterns in the mixture.

These findings collectively underscore the superior ability of the DES to isolate naphthalene from WMO, enabling selective extraction and purification. The integration of DFT and MD simulations provides a comprehensive understanding of the DES's molecular mechanisms, paving the way for designing more effective solvent systems. Future research should investigate alternative DES formulations, environmental impacts, and the recyclability of DESs to optimize contaminant removal and improve economic sustainability. This work contributes to advancing waste management technologies and the development of cleaner energy solutions.

Acknowledgement

This work was supported by the Committee of Science of the Ministry of Education and Science of the Republic of Kazakhstan via grant #AP25795799. This work was also supported by the Committee of Science of the Ministry of Education and Science of the Republic of Kazakhstan via grant #AP19676626.

Conflict of Interest

There is no conflict of interest.

Supporting Information

Not applicable.

References

[1] Q. Hassan, P. Viktor, T. J. Al-Musawi, B. Mahmood Ali, S. Algburi, H. M. Alzoubi, A. Khudhair Al-Jiboory, A. Zuhair Sameen, H. M. Salman, M. Jaszczur, The renewable energy role in the global energy Transformations, *Renewable Energy Focus*, 2024, **48**, 100545, doi: 10.1016/j.ref.2024.100545.

[2] D. K. Kushaliev, A. B. Zabieva, A. M. Balgynova, R. Burdzik, Z. R. Alipbaev, Diagnostics of an innovative repair kit for transport equipment units, *Diagnostyka*, 2024, **25**, 176291, doi: 10.29354/diag/176291.

[3] M. Amouei Torkmahalleh, M. Karibayev, D. Konakbayeva, M. M. Fyrillas, A. M. Rule, Aqueous chemistry of airborne hexavalent chromium during sampling, *Air Quality, Atmosphere & Health*, 2018, **11**, 1059-1068, doi: 10.1007/s11869-018-0607-z.

[4] C. S. H. Chen, J. J. Delfino, P. S. C. Rao, Partitioning of organic and inorganic components from motor oil into water, *Chemosphere*, 1994, **28**, 1385-1400, doi: 10.1016/0045-6535(94)90080-9.

[5] S. Abdulsalam, Bioremediation of soil contaminated with used motor oil in a closed system, *Journal of Bioremediation and Biodegradation*, 2012, **3**, 1-7, doi: 10.4172/2155-6199.1000172.

[6] M. A. Azevedo, M. dos R. Vieira-Neta, L. P. do Nascimento, G. F. da Silva, J. G. P. Vicente, I. C. S. Duarte, Potential brewer's spent grain as a carbon source alternative for biosurfactant production by Rhodotorula mucilaginosa (LBP4), *Journal of Environmental Chemical Engineering*, 2024, **12**, 111594, doi: 10.1016/j.jece.2023.111594.

[7] R. Maceiras, V. Alfonsín, F. J. Morales, Recycling of waste engine oil for diesel production, *Waste Management*, 2017, **60**, 351-356, doi: 10.1016/j.wasman.2016.08.009.

[8] M. Haghighat, N. Majidian, A. Hallajisani, M. Samipourgiri, Production of bio-oil from sewage sludge: a review on the thermal and catalytic conversion by pyrolysis, *Sustainable Energy Technologies and Assessments*, 2020, **42**, 100870, doi: 10.1016/j.seta.2020.100870.

[9] D. T. Kukwa, R. E. Ikyereve, E. O. Agbo, Cu and Ni mop up from spent lubrication oil using disposed plastic materials, *International Journal of Science and Engineering Applications*, 2014, **3**, 87-93, doi: 10.7753/ijsea0304.1005.

[10] O. Arpa, R. Yumrutas, A. Demirbas, Production of diesel-like fuel from waste engine oil by pyrolitic distillation, *Applied Energy*, 2010, **87**, 122-127, doi: 10.1016/j.apenergy.2009.05.042.

[11] M. A. Dos Reis, M. S. Jeronimo, Waste lubricating oil rerefining by extraction-flocculation. 1. A scientific basis to design efficient solvents, *Industrial & Engineering Chemistry Research*, 1988, **27**, 1222-1228, doi: 10.1021/ie00079a023.

[12] A. U. Abuova, Y. A. Mastrikov, E. A. Kotomin, S. N. Piskunov, T. M. Inerbaev, A. T. Akilbekov, First-principles modeling of oxygen adsorption on Ag-doped $LaMnO_3$ (001) surface, *Journal of Electronic Materials*, 2020, **49**, 1421-1434, doi: 10.1007/s11664-019-07814-2.

[13] S. J. Jensen, T. M. Inerbaev, A. U. Abuova, D. S. Kilin, Spin unrestricted nonradiative relaxation dynamics of cobalt-doped anatase nanowire, *The Journal of Physical Chemistry C*, 2017, **121**, 16110-16125, doi: 10.1021/acs.jpcc.7b04263.
[14] A. Shishov, S. Savinov, N. Volodina, I. Gurev, A. Bulatov, Deep eutectic solvent-based extraction of metals from oil samples for elemental analysis by ICP-OES, *Microchemical Journal*, 2022, **179**, 107456, doi: 10.1016/j.microc.2022.107456.
[15] D. Z. Troter, Z. B. Todorović, D. R. Đokić-Stojanović, O. S. Stamenković, V. B. Veljković, Application of ionic liquids and deep eutectic solvents in biodiesel production: a review, *Renewable and Sustainable Energy Reviews*, 2016, **61**, 473-500, doi: 10.1016/j.rser.2016.04.011.
[16] O. Ismagambetov, N. Aldiyarov, N. Almas, I. Irgibaeva, Z. Baitassova, S. Piskunov, A. Aldongarov, O. Abdirashev, Atomistic modeling of natural gas desulfurization process using task-specific deep eutectic solvents supported by graphene oxide, *Molecules*, 2024, **29**, 22, doi: 10.3390/molecules29225282.
[17] P. K. Naik, M. Mohan, T. Banerjee, S. Paul, V. V. Goud, Molecular dynamic simulations for the extraction of quinoline from heptane in the presence of a low-cost phosphonium-based deep eutectic solvent, *The Journal of Physical Chemistry B*, 2018, **122**, 4006-4015, doi: 10.1021/acs.jpcb.7b10914.
[18] D. Shah, D. Gapeyenko, A. Urakpayev, M. Torkmahalleh, Molecular dynamics simulations on extractive desulfurization of fuels by tetrabutylammonium chloride based deep eutectic solvents, *Journal of Molecular Liquids*, 2019, **274**, 254-260, doi: 10.1016/j.molliq.2018.10.131.
[19] A. H. Al-Marzouqi, A. Y. Zekri, A. A. Azzam, A. Y. Alraeesi, Optimization of supercritical fluid extraction of hydrocarbons from a contaminated soil: an experimental approach, *International Journal of Environmental Science and Development*, 2019, **10**, 301-309, doi: 10.18178/ijesd.2019.10.10.1191.
[20] A. Patel, B. Agrawal, B. R. Rawal, Pyrolysis of biomass for efficient extraction of biofuel, *Energy Sources, Part A: Recovery, Utilization, and Environmental Effects*, 2020, **42**, 1649-1661, doi: 10.1080/15567036.2019.1604875.
[21] M. M. Rahman, M. Akter, A. B. Siddik, M. W. Islam, S. Afrin, M. Afroze, M. Khan, M. A. Hoque, M. Al Mamun, Purification of waste engine oil using raw clay, acid treated clay and clay/activated charcoal, *Journal of Bangladesh Academy of Sciences*, 2024, **48**, 121-134, doi: 10.3329/jbas.v48i1.70241.
[22] P. M. Álvarez, J. Collado Contreras, S. Nogales-Delgado, Biodiesel and biolubricant production from waste cooking oil: transesterification reactor modeling, *Applied Sciences*, 2025, **15**, 575, doi: 10.3390/app15020575.
[23] M. Usman, M. Abraz, T. Ahmad, F. Riaz, F. Rehman, N. Hayat, Y. Fouad, F. Javed, M. A. Mujtaba, M. A. Kalam, Optimization of diesel engine characteristics using p-toluene sulfonic acid catalyst-based biodiesel from waste chicken fat oil, *Alexandria Engineering Journal*, 2025, **116**, 62-72, doi: 10.1016/j.aej.2024.12.086.
[24] A. H. Khan, N. Batool, A. Aziz, Recovery of base oil from used oil through solvent extraction followed by adsorption: a review, *Environmental Protection Research*, 2023, **3**, 319-340, doi: 10.37256/epr.3220232592.
[25] D. Hu, Q. Wang, X. Wang, T. Li, J. Li, Y. Chen, T. Ban, Y. Zhang, N. Yalikun, Experimental and mechanistic investigation of amide-based deep eutectic solvents for quinoline extraction and separation from wash oil, *Industrial & Engineering Chemistry Research*, 2024, **63**, 5397-5410, doi: 10.1021/acs.iecr.3c04327.
[26] S. A. Marquis Jr, E. A. Smith, Assessment of ground-water flow and chemical transport in a tidally influenced aquifer using geostatistical filtering and hydrocarbon fingerprinting, *Groundwater*, 1994, **32**, 190-199, doi: 10.1111/j.1745-6584.1994.tb00633.x.
[27] M. Karibayev, D. Shah, Comprehensive computational analysis exploring the formation of caprolactam-based deep eutectic solvents and their applications in natural gas desulfurization, *Energy & Fuels*, 2020, **34**, 9894-9902, doi: 10.1021/acs.energyfuels.0c01721.
[28] Gaussian 09, Revision A.02, M. J. Frisch, G. W. Trucks, H. B. Schlegel, G. E. Scuseria, M. A. Robb, J. R. Cheeseman, G. Scalmani, V. Barone, G. A. Petersson, H. Nakatsuji, X. Li, M. Caricato, A. Marenich, J. Bloino, B. G. Janesko, R. Gomperts, B. Mennucci, H. P. Hratchian, J. V. Ortiz, A. F. Izmaylov, J. L. Sonnenberg, D. Williams-Young, F. Ding, F. Lipparini, F. Egidi, J. Goings, B. Peng, A. Petrone, T. Henderson, D. Ranasinghe, V. G. Zakrzewski, J. Gao, N. Rega, G. Zheng, W. Liang, M. Hada, M. Ehara, K. Toyota, R. Fukuda, J. Hasegawa, M. Ishida, T. Nakajima, Y. Honda, O. Kitao, H. Nakai, T. Vreven, K. Throssell, J. A. Montgomery, Jr., J. E. Peralta, F. Ogliaro, M. Bearpark, J. J. Heyd, E. Brothers, K. N. Kudin, V. N. Staroverov, T. Keith, R. Kobayashi, J. Normand, K. Raghavachari, A. Rendell, J. C. Burant, S. S. Iyengar, J. Tomasi, M. Cossi, J. M. Millam, M. Klene, C. Adamo, R. Cammi, J. W. Ochterski, R. L. Martin, K. Morokuma, O. Farkas, J. B. Foresman, D. J. Fox, Gaussian, Inc., Wallingford CT, 2016.
[29] D. F. Tegegn, H. Z. Belachew, A. O. Salau, DFT/TDDFT calculations of geometry optimization, electronic structure and spectral properties of clevudine and telbivudine for treatment of chronic hepatitis B, *Scientific Reports*, 2024, **14**, 8146, doi: 10.1038/s41598-024-58599-2.
[30] F. Zhang, H. Li, X. Zou, C. Cui, Y. Shi, H. Wang, F. Yang, Performance and simulation study of aged asphalt regenerated from waste engine oil, *Coatings*, 2022, **12**, 1121, doi: 10.3390/coatings12081121.
[31] I. Y. Zhang, J. Wu, X. Xu, Extending the reliability and applicability of B3LYP, *Chemical Communications*, 2010, **46**, 3057, doi: 10.1039/c000677g.
[32] M. D. Wodrich, C. Corminboeuf, P. von Ragué Schleyer, Systematic errors in computed alkane energies using B3LYP and other popular DFT functionals, *Organic Letters*, 2006, **8**, 3631-3634, doi: 10.1021/ol061016i.
[33] A. K. Malde, L. Zuo, M. Breeze, M. Stroet, D. Poger, P. C. Nair, C. Oostenbrink, A. E. Mark, An automated force field topology builder (ATB) and repository: version 1.0, *Journal of Chemical Theory and Computation*, 2011, **7**, 4026-4037, doi:

10.1021/ct200196m.
[34] N. Schmid, A. P. Eichenberger, A. Choutko, S. Riniker, M. Winger, A. E. Mark, W. F. van Gunsteren, Definition and testing of the GROMOS force-field versions 54A7 and 54B7, *European Biophysics Journal*, 2011, **40**, 843-856, doi: 10.1007/s00249-011-0700-9.
[35] D. Shah, M. Karibayev, E. K. Adotey, M. Amouei Torkmahalleh, Impact of volatile organic compounds on chromium containing atmospheric particulate: insights from molecular dynamics simulations, *Scientific Reports*, 2020, **10**, 17387, doi: 10.1038/s41598-020-74522-x.
[36] P. Podio-Guidugli, On (Andersen-) parrinello-rahman molecular dynamics, the related metadynamics, and the use of the cauchy-born rule, *Journal of Elasticity*, 2010, **100**, 145-153, doi: 10.1007/s10659-010-9250-0.
[37] H. J. C. Berendsen, Transport properties computed by linear response through weak coupling to a bath, in Computer Simulation in Materials Science, Dordrecht: Springer Netherlands, 1991, 139-155, ISBN: 978-94-010-5598-2.
[38] D. Van Der Spoel, E. Lindahl, B. Hess, G. Groenhof, A. E. Mark, H. J. C. Berendsen, GROMACS: Fast, flexible, and free, *Journal of Computational Chemistry*, 2005, **26**, 1701-1718, doi: 10.1002/jcc.20291.
[39] P. Li, Z. Zhang, X. Zhang, K. Li, Y. Jin, W. Wu, DES: their effect on lignin and recycling performance, *RSC Advances*, 2023, **13**, 3241-3254, doi: 10.1039/d2ra06033g.
[40] D. Rodríguez-Llorente, A. Cañada-Barcala, S. Álvarez-Torrellas, V. I. Águeda, J. García, M. Larriba, A review of the use of eutectic solvents, terpenes and terpenoids in liquid-liquid extraction processes, *Processes*, 2020, **8**, 1220, doi: 10.3390/pr8101220.
[41] K. Shahbaz, F. S. Mjalli, M. A. Hashim, I. M. AlNashef, Using deep eutectic solvents based on methyl triphenyl phosphunium bromide for the removal of glycerol from palm-oil-based biodiesel, *Energy & Fuels*, 2011, **25**, 2671-2678, doi: 10.1021/ef2004943.
[42] A. J. Hussain, Z. S. Al-Khafaji, I. Q. Al Saffar, New recycling method of lubricant oil and the effect on the viscosity and viscous shear as an environmentally friendly, *Open Engineering*, 2024, **14**, 20220521, doi: 10.1515/eng-2022-0521.
[43] K. Babaremu, A. Adediji, N. Olumba, S. Okoya, E. Akinlabi, M. Oyinlola, Technological advances in mechanical recycling innovations and corresponding impacts on the circular economy of plastics, *Environments*, 2024, **11**, 38, doi: 10.3390/environments11030038.
[44] A. Mannu, S. Garroni, J. Ibanez Porras, A. Mele, Available technologies and materials for waste cooking oil recycling, *Processes*, 2020, **8**, 366, doi: 10.3390/pr8030366.